MMA Memo 83

THERMAL CONSIDERATIONS FOR mmA ANTENNAS

James W Lamb
5 May, 1992

1 Introduction

As an open facility the mmA is expected to be heavily scheduled and it is reasonable to expect it to perform within specifications even during the rapid temperature changes which occur on a clear exposed site at dawn and dusk. Furthermore, solar observing is specified as a major capability of the instrument, so special precautions need to be taken to allow high-precision operation during and after pointing at the sun, as well as avoiding damage by the focused IR and visible radiation. This note summarizes and supplements existing information on thermal problems from a variety of sources, and outlines areas to be studied.

A glance at a von Hoerner diagram for telescope structural limits shows that the thermal design of the mmA antennas is of critical importance [1]. The antenna specifications place them close to the limits predicted for a steel structure, for gravitational bending as well as thermal distortion. von Hoerner's calculations were based on a simplified model with assumptions about temperature gradients, etc., so it is necessary to look at the thermal performance in more detail to determine whether special materials or

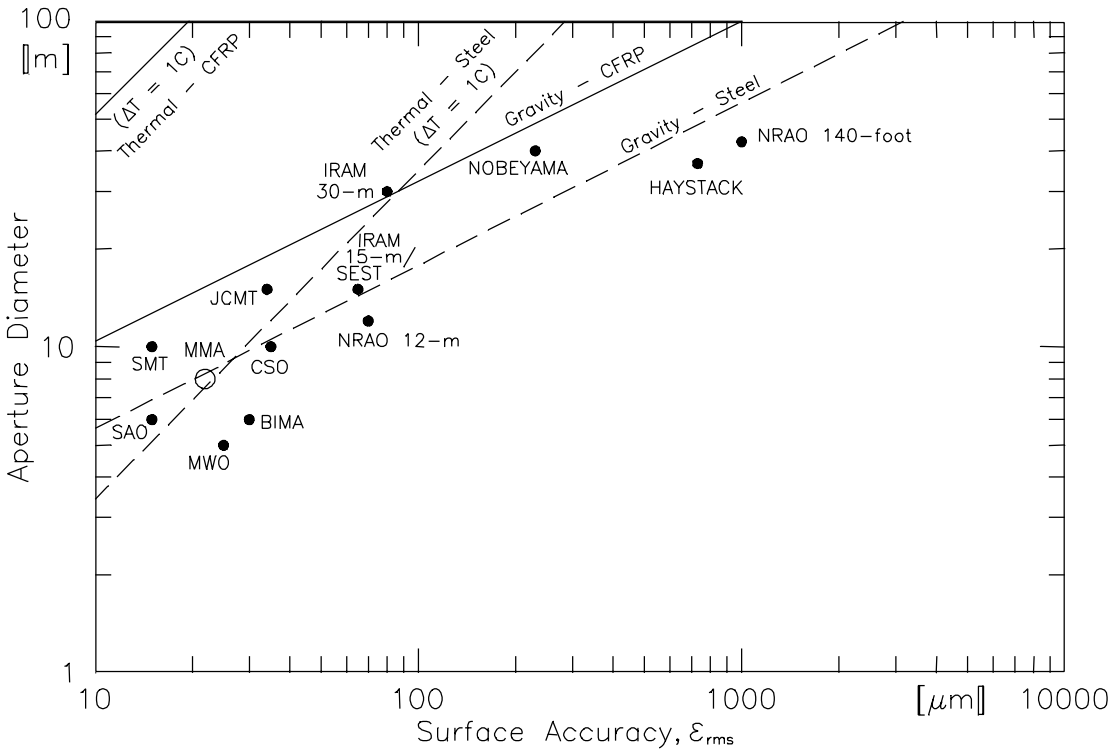

Figure 1 von Hoerner diagram showing achievable surface accuracies as limited by thermal and gravitational effects.

thermal controls will be required. Of the instruments listed in Fig. 1, the ones which surpass the thermal limit are: the IRAM 30-m, which has thermal controls, the JCMT, which is in an enc losure with adjustable louvers; the SMT which uses carbon fiber and an enclosure; and the SAO, which will probably use carbon fiber. Note that of the last two, the SMT is still under construction and the SAO antennas are in the design stage.

2 Design Options

In principle, it is possible to achieve very good immunity to thermal problems by using low thermal expansion materials such as Carbon Fiber Reinforced Plastic (CFRP). Practical constraints (primarily cost) dictate the use of other materials, however, so the intrinsic thermal performance will be compromised. To meet the specifications other methods of counteracting the thermal errors may be required.

Table I lists some of the design approaches to the thermal questions. The basic design should be made as good as possible within reasonable cost constraints. Although cost will limit the use of low expansion materials, judicious use of these along with suitable insulation and minimization of solar heating could be used to approach the design specifications.

If CFRP is not used further improvement of performance to meet the specifications with either temperature control or active compensation of distortions will probably required. Controlling the temperature could be expensive and complex, but circulation of air to minimize gradients is a possibility. Other options such as removing pointing and focus components of the errors are virtually cost-free, but

Strategy	Methods	Comments	Cost
Basic Design	☐ $\alpha \approx 0$	Special materials (Invar, CFRP)	V. High
	☐ Insulation	Affects time constants, temperatures	Low
	☐ Radiation Control	Paint, Foil	Low
	☐ Enclosure	Hard to transport, pack together	High
Active Temperature Control	☐ Circulation	Fans, ducts, cladding	Low
	☐ Heaters	High Power consumption	Low
Measurement of Errors	☐ Radiometric	Periodic, Interrupts observing	Low
	☐ Ancillary Instr.	Continuous, Needs development	Mod.
Compensation	☐ Active Surface	Complex, Potentially unreliable	High
	☐ Re-pointing	No extra hardware required	Low
	☐ Re-focusing	No extra hardware required	Low

Table I Strategies for meeting specifications of the antennas under expected thermal conditions.

compensation of these errors requires that they be measured first. Radiometric measurements will be required periodically under any circumstances for atmospheric calibration and can yield information on pointing, focus, etc., but direct measurements of the structure will probably be needed to interpolate between or replace some of the astronomical calibrations, as well reducing their frequency and duration, to maintain the highest precision.

Once the errors are measured corrections can be applied. In principle small-scale distortions can be corrected with an active mirror, but the high cost and reliability questions make this very undesirable and such errors should be guaranteed small by the fundamental design. Large-scale errors can be compensated by re-pointing and re-focusing using mechanisms which will be on the antenna anyway. The challenge lies in developing suitable instrumentation and relating the measurements to focus and pointing models.

3 General Considerations

For the present it will be assumed that the antennas will be operated without any enclosure and will be exposed to the full sun and extreme temperatures. On a typical site the temperatures may be expected to vary by as much as 20 C daily and 50 C annually. As well as changes in absolute temperature there will be gradients within the antenna structure and differences in temperature between antennas, particularly when they are in the large configurations. In the compact configurations the thermal environment of one antenna may be influenced by neighboring ones by shadowing of the sun or shading from wind.

3.1 Materials

The materials which are likely to be considered for major structural parts are listed in Table II along with some relevant thermal data. CFRP and Invar both have very low thermal expansion coefficients, but their expense will limit their use to critical parts of the structure. An attractive feature of CFRP is the possibility of tailoring its properties for different applications. Aluminum has a high thermal expansion coefficient, but its electrical properties make it desirable for the reflector surface. Steel has

Property	ASTM A36 Carbon Steel	6061-T6 Aluminum	Carbon-Fiber-Reinforced-Plastic	Invar
Density, ρ ($kg\ m^{-3}$)	7 860	2 700	1 600	8 000
Specific Heat, c_p ($J\ kg^{-1}\ C^{-1}$)	418	962	710	503
Thermal Expansion Coefficient, α ($\times 10^{-6}\ C^{-1}$)	12.7	23.0	0 - 4	0.9
Thermal Conductivity, k ($W\ m^{-1}\ C^{-1}$)	52	17.2	4.2	16

Table II Thermal properties of suitable structural materials.

moderate expansion coefficient and conductivity, and its cost, availability and general suitability mean that it should be used in major structural components, such as the mount.

3.2 Heat Sources and Sinks

Solar radiation, which has a maximum flux of about 1.2 kW m^{-2}, is the major heat source. Generally the solar flux on the antenna surfaces will be lower than this because of atmospheric absorption and angle of incidence. Radiated heat to or from ambient will be proportional to the temperature difference, ΔT, between the structure, T_s, and the surroundings, T_0.

$$q = 4\sigma T_0^3 \Delta T \tag{1}$$

where σ is Stephan's constant. For a black body at T_0 = 290 K this corresponds to about 5.5 W m^{-2} C^{-1} and will be less for materials with lower emissivity. Radiation to the sky will be larger since the atmosphere is relatively transparent at λ 10 mm where the peak in the 300 K black-body spectrum lies. Convective heat transfer is dependent on the geometry and orientation of the structure. Natural convection is proportional to $\Delta T^{1\ 1/3}$, while forced convection is proportional to ΔT. Typical cooling rates are of the order of 2-10 W m^{-2} C^{-1}, comparable to the radiative transfer rates to ambient, but the actual value is dependent on the, wind, and temperature.

Another significant source of heat is the dissipation from compressors, air-conditioning units, and electronics, which will amount to several kW.

3.3 Absolute Temperature Effects

Some degradation in performance will result when the mean temperature of the structure changes from that at which the surface was adjusted, or from the temperature at the last calibration of pointing, phase, or focus. Pathlength changes will depend on the thermal expansion coefficients, α, of the materials used, while surface accuracy will depend on differences between expansion coefficients of different materials. Pointing will be unaffected in a symmetrical antenna. Expansion coefficients for several typical materials are given in Table II. Values of α are around 10^{-5} C^{-1} so that a structure of order 10 m will experience pathlength changes of about 100 mm C^{-1}. Temperature differences between antennas should not vary by more than about 0.1 C hr^{-1} to maintain phase stability of better than 10 mm hr^{-1}

3.4 Temperature Gradients

Temperature gradients can have severe effects on pointing and surface accuracy. The effects will be proportional to the expansion coefficients, α, and temperature gradients, ∇T.

3.5 Thermal Time Constants

Thermal time constants characterize the rate at which heat is distributed through or removed from a body. An intrinsic time constant, τ_i may be defined which describes the rate of change of temperature of a body when it is limited by the thermal conductivity of the material. For a body of characteristic size L_c , thermal conductivity κ, density ρ , and specific heat c_p, τ_i is given by [2]

$$\tau_i = \frac{\rho c_p L_c^2}{4\kappa} \tag{2}$$

When the rate of change is governed by the rate, h, at which heat can be removed from the body an extrinsic time constant, τ_e, can be defined as

$$\tau_s = \frac{\rho c_p L_c}{h} \tag{3}$$

When $\tau_e \gg \tau_i$ the overall time constant is independent of the thermal conductivity of the material. This will be true when

$$L_c << \frac{4k}{h} \tag{4}$$

For a heat transfer coefficient of 4 W m^{-2} C^{-1} the right hand side is about 50 m for steel and 5 m for CFRP.

3.6 Analysis

It is convenient to break the antenna down into parts for analysis: mount, backing structure, primary surface, secondary reflector and its support. These can be considered individually but their mutual influences also have to be studied. In a properly designed structure the interactions between major components should be minimized and well defined.

4 Mount

Steel is the preferred material for the mount, though it has a moderately high expansion coefficient of $\alpha_{steel} = 12\times10^{-6}$ C^{-1}. Uniform temperature changes produce pathlength changes, while gradients cause pointing offsets. If the mount has a height h and width w then the tilt for a temperature change ΔT is approximately

$$\beta = \frac{\alpha_{steel} h \Delta T}{w} \approx \frac{2.5 h \Delta T}{w} \quad [arcsec] \quad for\ steel \tag{5}$$

Typically $h \gg w$ so that temperature differentials need to be less than 0.1 C to keep the pointing offset less than 0.25 arcsec. Clint Janes has measured temperature distributions on VLA and VLBA antennas using an IR camera [3]. He measured 4 to 5 C differences vertically in the yoke on a VLA antenna, and 0.25 C along a beam at the base of a VLBA antenna. While those antennas are considerably larger than the proposed mmA design, the results give an estimate of the magnitude of the gradients which can exist. Bregman and Casse [4] predicted temperature differences of 22 C across the JCMT design if it were unenclosed with no insulation. This would drop to 5.1 C with appropriate insulation. Clearly, to make the mount intrinsically accurate will involve very careful precautions to keep the temperature uniform.

Uniformity may be achieved by minimizing the heat flux into and out of the mount and by making the time constant long compared to the rate of change in heating by the sun, etc. The thermal time constant for heat to be transferred from one side of the structure to the other is approximately

$$\tau_i = \frac{\rho c_p w^2}{4k_{steel}} \tag{6}$$

where ρ and c_p are for steel. If w = 4 m this gives t_i = 3.3 day, so that the structure will never come close to equilibrium during the diurnal solar heating cycle if one side of the mount is significantly heated. The time it takes to heat one side of the structure through a layer of insulation with thermal conductivity k_{ins}, and thickness t_{ins} is about

$$t_s = \frac{\rho c_p t_s t_{ins}}{k_{ins}} \tag{7}$$

where t_s is the thickness of the steel members, Taking t_s = 13 mm and k_{ins} = 0.05 W m^{-1} C^{-1} indicates that the insulation thickness should be about 350 mm with a corresponding heat transfer rate of 0.14 W m^{-2} C^{-1}.

Alternatively, some pointing deviations can be accepted provided that they are calibrated out by some means. If β is to be predicted from temperature measurements then the average ΔT also needs to be known to an accuracy of about 0.1 C. A brief look at commercial temperature sensors shows that resolutions of this order are typical, although accuracy is generally a few tenths of a kelvin. Probably a few (e.g. 4-8) sensors would be used on each side of the mount so that the effect of statistical variations will be reduced. Thermistors with tolerances of ±0.05% over a range of 50 C are available, so this method seems feasible.

Another possibility is to measure the relative movements of the structure directly using lasers, or CFRP rods as temperature stable distance measures. The end of the rod would have a displacement transducer which would measure the relative motion of part of the structure. This would require a length measurement accuracy of

$$\Delta l = w\beta \tag{8}$$

For β = 0.25 arcsec and w = 2 m, Δl will be 2.5 mm. The range would be

$$R = h\alpha\Delta T \tag{9}$$

which for ΔT = 50 C, h = 2 m, α = 12×10^{-6} C^{-1} is 1.2 mm, giving a dynamic range of 500. This accuracy and range is achievable with an LVDT, for example.

Tilts may also be measured directly with a commercial electronic tiltmeter. If these devices are placed above the azimuth bearing, radial forces due to tracking at sidereal rates will give errors of order 10^{-4} arcsec which is quite negligible, but settling times after slewing may be a problem. The tiltmeter should be located as close to the azimuth axis as possible to minimize this.

Temperature differences between antennas will introduce a differential pathlength error. This will be calibrated out if it is constant, but could be important if it is variable. To hold the rate of change of pathlength below 10 mm hr^{-1} the differential rate of temperature change between antennas must be less than about 0.2 C hr^{-1}. This will depend on the topography as well as the antenna design. If the mount time constant is made sufficiently long it may not be a problem.

5 Backing Structure

There are several approaches to minimizing the thermal effects in the backing structure. These

may be divided into three groups. (a) the structure may be made insensitive to temperature changes and gradients (e.g. the SMT which uses CFRP with a very low expansion coefficient), (b) the temperature gradients (and/or temperature) may be controlled to a high degree (e.g. IRAM 30-m antenna has fans in the backing structure and active thermal control of the secondary mirror support legs), or (c) a combination of (a) and (b). In addition, measurements of temperature or position on the structure will allow compensation of some of the focusing and pointing terms. Another form of thermal control is to use

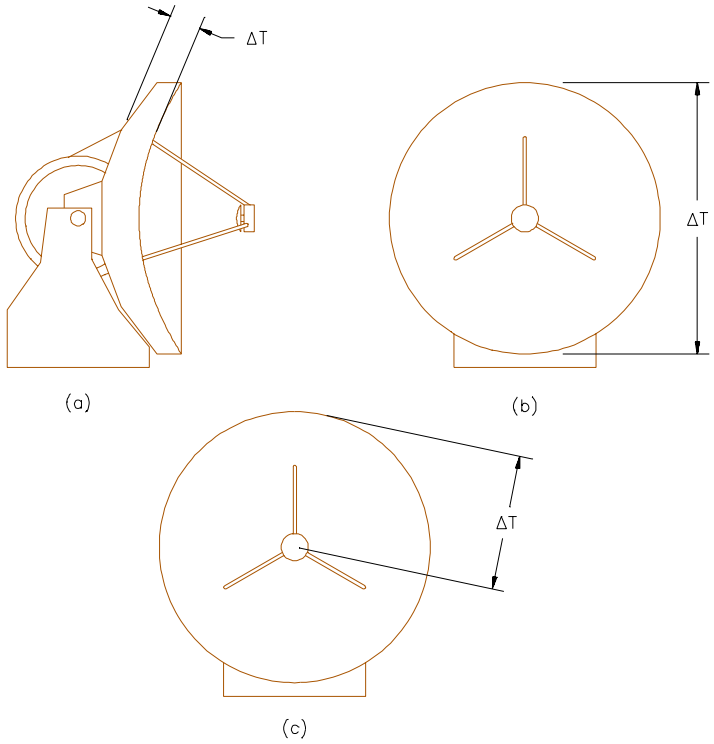

Figure 2 Temperature distributions considered in text. *a*. Front-to-rear, *b*. Top-to-bottom, *c*. Radial.

an enclosure, such as a radome or astrodome. For the present we will ignore the possibility of an enclosure because of the added difficulties in transportation and close-packing of antennas.

Space frames appear to be the best choice for backing structures. These are relatively simple to analyze accurately and can easily be made from combinations of different materials such as CFRP and steel. This type of structure will be assumed in the following discussion.

5.1 Estimates of Distortions

To get some understanding of whether an active temperature control system is required for the mmA we need to estimate the magnitude of some of the thermal effects. Some elementary calculations have been done using the model in Fig. 2*a* for the backing structure. A radial rib is represented as a plane lattice framework, where the expansion coefficients of the radial and transverse members are allowed to be different, α_r, and α_t, respectively. A gradient from the front to the back of the reflector tends to warp it as shown in Fig. 2*b*, while gradients along the rib will tend to cause a change in thickness (Fig. 2 *c*). Local inhomogeneities can potentially have quite damaging effects as they affect large parts of the structure through some type of lever action. The size scale of these is such that refocusing or repointing cannot

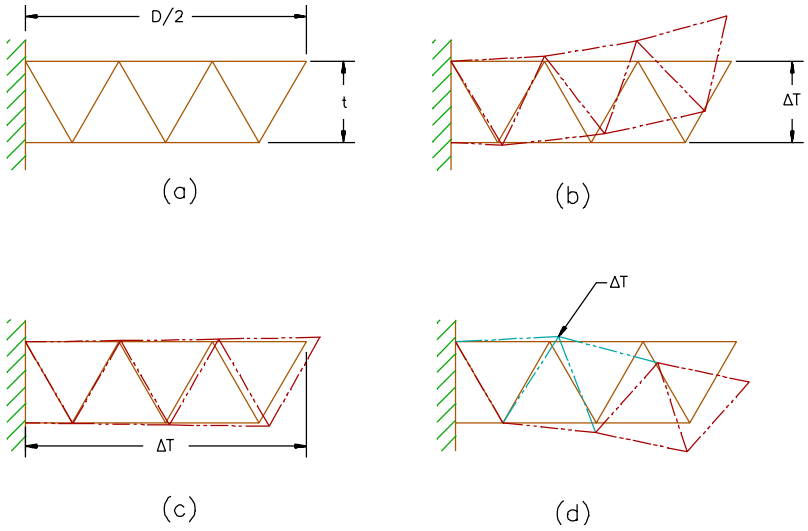

Figure 3 Model structure used in the calculations. *a*. Undistorted, *b*. Gradient through rib, *c*. Gradient along rib, *d*. Local gradient.

remove them. Several specific cases are now considered.

Fig. 3 shows the temperature distributions over the reflector which will be considered along with the appropriate distribution from Fig. 2.

Case I: Assume a linear gradient, ΔT, from the front to the rear of the reflector (Fig. 2*b*, Fig. 3*a*). This causes the rib to bend and produces a focus change of

$$\frac{\Delta f}{f} = \frac{2 f \alpha_r \Delta T}{t} \tag{10}$$

without any degradation to the surface accuracy. If the time-constant of the change is short compared to the interval between focus checks there will be a focusing loss which will be roughly equivalent to a degradation of surface accuracy of

$$\varepsilon_{eff} \approx \frac{0.02}{(f/D)^2} \Delta f \tag{11}$$

Of course, the movement of the secondary must also be considered, and it may increase or decrease this depending on the temperature distribution and properties of the support legs.

As a check, take the following numbers as being representative of the SAO 6-m design [5]. f = 2.5 m, t = 0.7 m, $\alpha_r = \alpha_{CFRP+steel} = 3\times10^{-6}$ C^{-1}, ΔT = 2 C. This yields Δf = 110 mm which compares favorably with the finite element analysis value of 54 mm, considering the simplifications used. For numbers more appropriate to the mmA take f = 3.2 m, t = 1 m, $\alpha_r = 12\times10^{-6}$ C^{-1} for which the change in focal length of the primary is Δf = 250 mm C^{-1}. If the secondary mirror is not refocused this leads to an equivalent surface error of ε_{eff} = 30 mm C^{-1}. Replacement of the steel with CFRP could reduce this by a factor of 4 to 8.

Case II: Assume a linear temperature gradient of $\Delta T/D$ across the aperture, Fig. 2*c*, Fig. 3*b*. To a first approximation this induces a beam squint of

$$\Delta\theta = \frac{\alpha_t t \Delta T}{2D} \tag{12}$$

with no contribution to the surface error. For the SAO design $\alpha_t = 12\times10^{-6}$ C^{-1}, t = 0.7 m, ΔT = 2 C, and D = 6 m, so that $\Delta\theta$ = 0.3 arcsec which is of the same order as the finite element analysis value of 0.7 arcsec. Using $\alpha_t = 12\times10^{-6}$ C^{-1}, t = 1 m, D = 8 m gives $\Delta\theta$ = 0.75 arcsec C^{-1}.

Case III: Assume a linear radial gradient of $2\Delta T/D$ along all the ribs, Fig. 2*c*, Fig. 3*c*. This produces a focusing error of approximately

$$\frac{\Delta f}{f} = 10\frac{f t \alpha_t \Delta T}{D^2} \tag{13}$$

and an rms surface error which is of order

$$\varepsilon = \frac{\alpha_t t \Delta T}{40\sqrt{2}} \tag{14}$$

Taking $\alpha_t = 12\times10^{-6}$ C^{-1}, t = 1 m, f = 3.2 m, D = 8 m, gives Δf = 18 mm and ε = 0.2 mm C^{-1}. With no refocusing there would be an additional equivalent surface error of ε_{eff} = 2 mm C^{-1}.

It is clear, then, that these large scale distributions cause changes which can be largely removed by repointing or refocusing, provided that they can be calibrated either astronomically or by ancillary instrumentation. Obviously there will be higher order terms which are not represented in this analysis but which will appear in a numerical model of a specific structure. This analysis should at least give some kind of upper bound on those terms, which will probably be an order of magnitude smaller. More complicated temperature distributions, such as shown in Fig. 2*d*, cannot be easily analyzed analytically, but it may be expected that these would produce more severe distortions of the surface figure. In general, the smaller the spatial scale of the temperature gradients the less effect on pointing and the greater the effect on the surface accuracy so that local sources of heating should be avoided.

The primary heat sources for the backing structure are direct solar radiation, indirect solar heating *via* the panels, ground radiation, and dissipation from compressors, electronics, etc. The interactions between these can be manipulated to some extent. For example, it will be worthwhile looking at treatment of the rear of the panels and selection of panel mount conductance so that the backing structure is heated uniformly by convection and radiation from the panel rear surface rather than locally at the mounting points. This will also ensure that there are no large gradients along a panel.

5.2 Thermal Time Constants

Generally the time constants of the structure will be determined by the heat capacity of the material and the rate at which heat can be removed from the members (the extrinsic time constant). Equation (3) can be used with the thickness of the members, t, as the characteristic length. All members should have a similar thickness to keep the time constants uniform. From this point of view the "box" type of structure, such as used on the NRAO VLA and 12-m antennas for the central part of the backing structure is preferable to the "strong ring" support used on the Bonn 100-m and the JCMT, for example. For typical values take a thickness of 4 mm and a heat transfer rate of 8 W m^{-2} K^{-1}. For steel this gives τ_e = 0.45 hr, and for CFRP, τ_e = 0.16 hr.

The time constants can also be used to estimate the spatial extent and distorting effects of local heating. Consider a part of the backing structure which is heated at one end at a rate q, such as a tube heated through a panel support. The heat will diffuse a distance l down the member in a time τ_i given by equation (2)

$$\tau_i = \frac{\rho c_p l^2}{4\kappa} \tag{15}$$

The rate at which heat is removed from the walls is given by the extrinsic time constant (equation (3)),

$$\tau_e = \frac{\rho c_p t}{h} \tag{16}$$

The temperature gradient along the member will be over a distance of order l_0, which is found by setting $\tau_e = \tau_i$ to give

$$l_0^2 = \frac{4\kappa t}{h} \tag{17}$$

For a thickness of 4 mm and heat flow h = 8 W m^{-2} K^{-1} this is 0.35 m and for CFRP it is 0.11 m. These relatively small scales indicate that the backing structure will come to equilibrium by exchanging heat with the surroundings rather than by conduction through the material itself. Over this distance the temperature change will be about

$$\Delta T = \frac{q}{p l_0 h} \tag{18}$$

where p is the perimeter distance of the tube, and the length change will be

$$\Delta l = \alpha \Delta T = \frac{\alpha q}{p\sqrt{4\kappa t h}} \tag{19}$$

Values obtained from this equation cannot be expected to be accurate, but it should at least be useful for comparing different materials. The ratio for two materials denoted by subscripts 1 and 2 is

$$\frac{\Delta l_1}{\Delta l_2} = \frac{\alpha_1}{\alpha_2}\sqrt{\frac{\kappa_2}{\kappa_1}} \tag{20}$$

For steel and CFRP this ratio is about unity, so that the relatively low thermal conductivity of the CFRP is not a disadvantage.

5.3 Expected Temperature Gradients

There is little detailed information on temperature distributions in antenna structures available, though there are some sources which give partial measurements. It should be noted that gradients need to be known with a resolution of 0.1 C or better. Akabane [6] reports some temperature distributions in the Nobeyama 45-m antenna which give average temperature gradients radially along the ribs of 0.13 C^{-1} m^{-1} (day time), and -0.09 C^{-1} m^{-1} (night time) with forced air circulation at a rate of about 1.5 m s^{-1} in the backing structure. In terms of an 8 m antenna this translates to about a 1 C gradient across the aperture which is not negligible. Akabane's data also show differences of 0.5 C (day) and 0.3 C (night) between the front and rear of the backing structure, also a significant amount. For these temperature distributions

the computed contribution to the surface error is 50 mm (day) and 30 mm (night). The temperature distribution is apparently not a simple gradient and there is some scatter among the nodes which were monitored. For example, there are a few nodes on the front surface which have the same temperature as those on the rear while most are significantly different. It is not stated what the accuracy of the measurements, but if it is not a calibration uncertainty then these nonuniformities probably contribute substantially to the surface error budget. Akabane also describes a 6 m diameter antenna of steel and aluminum which exhibits temperature differences of 20 C (day) and 5 C (night), leading to severe variations in the antenna efficiency.

Greve *et al.* [7] describe the thermal design of the IRAM 15-m and 30-m antennas. The 15-m antennas have a mixed CFRP/Steel backing structure with thermally insulating rear cladding. Individual sensor data are not given but differences between the averages of sensors on the upper half of the dish and the lower half vary from about 2 C at night to 12 C during the day. There are rms temperature variations of about 1 C at night and 2 - 3 C in the day. The 30-m antenna is steel with insulation and tangential airflow of several $m\,s^{-1}$. Variations in temperature with an rms between 0.3 C and 2 C were recorded in backing structure.

The above results demonstrate that even with active thermal control significant thermal gradients can exist within the backing structure. Diurnal variations are seen in all the measurements with most of the changes taking place over a couple of hours near sunrise and sunset. If the structure is thermally sensitive there will be significant focusing and pointing shifts which will reduce the antenna efficiency if they are not compensated for. Either temperature control or monitoring of the changes will be required if full accuracy is to be maintained over this period when the change is too rapid for focusing and point calibrations to be effective.

6 Panels

Several types of panel have been used or proposed for millimeterwave and sub-millimeterwave antennas. These include: aluminum skins with aluminum ribs epoxied on the rear (eg ESSCO panels on the 12-m, U. Mass Antennas); aluminum honeycomb with aluminum facings (eg JCMT); aluminum honeycomb with CFRP facings (eg SMT, IRAM 15-m); cast, machined aluminum (eg BIMA 6-m antennas); and CFRP honeycomb with CFRP facings. These all have different thermal properties which must be taken into account when choosing the type and dimensions of the panels.

Thermal effects may be divided into absolute temperature (T) effects, and gradient (ΔT) effects. These effects can be quite complex in detail and depend on the construction and materials of the panels, the method of mounting them, and the temperature distributions. Some simplifications can be used to estimate the relative merits of different panel types.

6.1 Absolute Temperature Effects

Consider first the absolute temperature effects. Clearly, if the panels and backing structure are made from the same material then a change in temperature will require (at most) refocusing the secondary. If there is a difference in temperature between the backing structure and the surface panels, or they have a different expansion coefficient the curvature of the panels will not match that of the backing structure and there will be a contribution to the surface error budget.

To estimate the magnitude of this effect, assume that the backing structure has a expansion coefficient of α_b, and that the panels are homogeneous and isotropic with a expansion coefficient of α_p.

Further assume that the panels are supported at their front surfaces at the edges and that the typical linear size of a panel is d_p. It may then be shown that the rms surface error is approximately

$$\varepsilon = \frac{\left|(T_p - T_0)\alpha_p - (T_b - T_0)\alpha_b\right|}{8\sqrt{3}R_0} d_p^2 \qquad (21)$$

T_p and T_b are the panel and backing structure temperatures and T_0 is the temperature at which the surface was set. R_0 is the panel radius of curvature (averaged over the sagittal and tangential directions) and depends on the focal length of the primary mirror.

For an 8 m diameter antenna with a focal ratio of 0.4 the radii of curvature at a 2 m radius on the aperture are 6.7 m and 7.4 m, so the average value is about $R_0 = 7$ m. For material expansion coefficients take $\alpha_{CFRP} = 2\times10^{-6}$ C^{-1}, $\alpha_{Al} = 23\times10^{-6}$ C^{-1}, $\alpha_{steel} = 12\times10^{-6}$ C^{-1}.

Case I: CFRP backing structure, aluminum panels.

$T_p = T_b = T_0 + 30$ C

then

$\varepsilon = 7$ mm $\times d_p^2$ $\quad$ d_p in m

eg 7 mm for a 1 m panel, 1.5 mm for a 0.5 m panel.

Case II: Steel backing structure, aluminum panels.

$T_p = T_b = T_0 + 30$ C

then

$\varepsilon = 2.5$ mm $\times d_p^2$ $\quad$ d_p in m

eg 2.5 mm for a 1 m panel, 0.6 mm for a 0.5 m panel.

Case III: Steel backing structure, aluminum panels.

$T_b = T_0$, $T_p = T_0 + 10$ C

then

$\varepsilon = 2.3$ mm $\times d_p^2$ $\quad$ d_p in m

eg 2.3 mm for a 1 m panel, 0.6 mm for a 0.5 m panel.

6.2 Gradient Effects

A thermal gradient between the front and back of the panel will cause it to warp. For a uniform

panel with an expansion coefficient of α_p the change in curvature is

$$c = \alpha \frac{\Delta T}{t} \tag{22}$$

For a given thermal flux, I, and thermal conductivity, κ, the temperature difference will be

$$\Delta T = \frac{It}{\kappa} \tag{23}$$

so that the curvature is

$$c = \frac{\alpha_p I}{\kappa} \tag{24}$$

i.e. *independent* of panel thickness. Table III shows values of α_p/κ for typical materials.

Material	α (C^{-1})	κ (m C^{-1})	α/κ (m^{-1})
Aluminum	23×10^{-6}	156	1.5×10^{-7}
CFRP	$0 - 5\times10^{-6}$	4.2	$0 - 12\times10^{-7}$
Carbon Steel	12×10^{-6}	52	2.3×10^{-7}
Invar	0.9×10^{-6}	16	5.6×10^{-8}

Table III Some thermal properties of common materials.

6.3 Estimated Gradients

It is difficult to make accurate estimates of actual temperature distributions, and numerical studies and measurements will be required for definitive answers. It is, however, possible to make some rough estimates of the thermal flux through a panel.

Assumptions are as follows: direct solar flux of 1.2 kW m^{-2}; emissivity for solar flux, 0.3; ambient temperature, 290 K; infra-red emissivity, 0.08. Heat input to the panel is from the solar flux on the front surface and radiation from ambient on the rear. Heat outflow is from thermal radiation and natural convection on both surfaces, and it is assumed that the conduction through the supports is about 0.5 W K^{-1}. With some reasonable assumptions about convective heat transport [8] the energy balance equation may be solved to yield a thermal flux through the panel of about 140 W m^{-2}.

For an aluminum panel of 1 m size the rms surface accuracy would be about 1.5 mm. If the panel has stiffening ribs on the rear the convective dissipation on the rear surface could increase with a corresponding increase in the gradient, though probably by a factor of only about 2 at most, which would still be acceptable. If the ribs were made separately and bonded using epoxy the thermal resistance at the

bond line could be a significant problem. A panel made from aluminum skins on an aluminum honeycomb will have an rms which is greater than that of a solid one by a factor *m*, where *m* is the inverse of the fractional filling of the aluminum in the honeycomb. Typically this may range from 10 to 80, so that this type of panel could be as bad as 15-120 mm. Unless a suitable surface treatment to reduce the solar absorption was used this construction must be ruled out as a possibility. Panels of mixed materials are hard to analyze, but for a crude estimate for CFRP panels with aluminum honeycomb assume that the expansion coefficient of the CFRP is modified by the aluminum to give the value estimated by Delannoy[9] to be about 4.5×10^{-6} C^{-1}, and the conductivity to be that of the aluminum honeycomb, which gives $\alpha/k = 2.9 \times 10^{-8} \times m$ m W^{-1}. The rms for a 1 m panel is then $0.3\times m$ mm. It is therefore comparable to a cast aluminum panel for $m \approx 5$. A CFRP panel with CFRP honeycomb would be perfect if α were adjusted to zero, but for $\alpha = 2\times10^{-6}$ C^{-1} the accuracy for a 1 m panel would be $2 \times m$ mm. Some current designs for CFRP panels have highly reflective surfaces so that the flux calculation given above will be an over estimate, and ε would be correspondingly smaller. It should also be remembered, however, that the high reflectivity is not necessarily desirable since much of the energy will be focused towards the secondary mirror and receiver optics during solar observations.

These estimates indicate that an aluminum panel is thermally good, possibly better than a CFRP or CFRP/aluminum-honeycomb one.

6.4 Gaps Between Panels

There will be gaps between panels partly to make mounting feasible, but also to allow for thermal expansion between the panels and the backing structure. If the backing structure is steel and the panels are aluminum the panel gap needs to be about 0.04% of the panel size for a 40 C change in temperature. For a 1 m panel this is about 0.4 mm, but practically the panels would probably be separated by at least 1 mm. This corresponds to an average scattering of about -24dB relative to isotropic.

7 Secondary Mirror Support

Changes in the temperature of the secondary mirror support temperature will lead to changes in pointing and focus. Depending on how the struts are attached to the secondary mirror mount and the backing structure or mount, differential thermal effects could potentially disrupt the surface figure but this may be avoided with careful design. If steel struts are used they would probably need to have air circulated to keep them at equilibrium with the backing structure. This would partially compensate for some of the changes in the backing structure shape with temperature. An alternative would be to make the struts from CFRP, which would be a relatively small part of the overall costs, and avoid the need for any forced circulation. Material with suitably high solar reflectivity would be required.

Shifts in pointing could also be monitored using a laser beam and a quadrant detector, as on the 12-m telescope. If it is possible to locate the quadrant detector behind the secondary, at its center of curvature, pointing offsets due to both lateral shifts and tilts would be measured. It would also be possible to measure the focus position relative to the primary by using a laser ranger such as that developed by J. Payne for the Green Bank Telescope [10]

8 Secondary Mirror

The secondary mirror is subjected to the same thermal gradient problems as the panels. In general the effect will be less as the secondary will generally be at an oblique angle to the sun. In addition, simple changes in curvature may be removed by re-focusing. An exception to this is for solar observing which is discussed more in detail below. Differences in temperature relative to the primary

mirror will cause some change in the focus. A difference of 10 C will change the focal length of the secondary by an amount of order 0.05 mm if the mirror is aluminum. This is probably negligible in most cases, especially as it will periodically be refocused.

8.1 Solar Observing

The requirement for observing the sun places heavy demands on the antenna. If the primary diameter is D, the secondary diameter d, the primary mirror reflectivity R, and the solar constant s = 1.2 kW m^{-2}, then the power density at the secondary will be

$$I_s = sR\left(\frac{D}{d}\right)^2 \tag{25}$$

Typically, D/d = 10 - 20, and R = 0.6 - 0.92, so that I_s = 72 - 450 kW m^{-2}. The effect on the secondary will depend on the reflectivity of the secondary mirror — if it is small the secondary will be severely affected and if it is large the energy will be transmitted to the receiver optics. Some of the solutions to investigate are to have small scale roughness on the primary to diffuse the power over a range of angles large compared to the angle subtended by the secondary as seen from the primary, or to use a membrane such as Goretex, which is transparent to mm-waves but has a high solar reflectance, over the receiver optics. Hills [11] and Welch [12] have both discussed the role of surface finish in scattering sunlight.

9 Site Dependence

Dependence of thermal effects on different sites is generally rather weak. The main factors are the air density, and the wind speeds which affect the convective cooling. For an extreme change of altitude from 2 km to 4 km the air density falls by about 27%. Natural convection depends on the kinematic viscosity and thermal conductivity of the air and the net difference in cooling between these altitudes is only about 20%. Forced convection is proportional to the thermal conductivity and changes by less than 5% between these altitudes. It is also proportional to $v^{-1/2}$, where v is the wind speed. Considering that the range of elevations of the possible sites is smaller than this it is clear that the site dependence of thermal effects is small compared to the accuracy of the modeling.

A site-dependent effect which could be of importance is the uniformity of temperature variation over the array (particularly in the large configuration), as this will affect the relative phase stability of the antennas.

10 Conclusions

The concept of a simple, reliable, cheap antenna is very attractive. Fabrication using CFRP extensively could satisfy the first two attributes but will probably be relatively expensive, so the limits of more conventional materials have to be investigated in depth.

Clearly there is much to be understood about the thermal design. The mount can probably be well understood and appropriate steps taken to minimize or compensate for thermal effects. Even if gradients cannot be eliminated, the time constant could be made long enough that they are not a problem, Proper account needs to be taken of heating by electronics, compressors, etc.

Analysis of the backing structure is much more complex. To meet the specifications without any compensation for thermal distortions with a steel construction requires thermal gradients across the aperture to be less than a few tenths of a degree Celsius. However, many of the gross thermal effects can

be viewed as changes in pointing or focusing and if these can be calibrated or monitored in real time the ultimate limitation becomes the effect of the residuals on the surface accuracy. This relaxes the temperature uniformity needs and it is then not clear that a steel backing structure cannot meet the specifications, even without control of forced circulation.

If the thermal time constants are on the order of an hour, astronomical calibrations may not always be frequent enough to remove the systematics, and supplementary instrumentation will be required. Time constants in the backing structure will probably be short (0.1-1 hr) and the changes will be determined by the ambient conditions (0.1-24 hr). Enclosure of the backing structure may increase the time constant, but it might then be necessary to install fans to ensure that no stratification occurs within the enclosure. The mount will have much longer time constants than the backing structure, so it is important to decouple these effectively.

Thermal considerations for panels rule out the aluminum-aluminum honeycomb-aluminum construction but otherwise is not very restrictive on construction. The choice will be based more on cost, and gravitational and wind loading deflections.

Although it is relatively easy to compute what a given temperature distribution has on the structure it is very difficult to predict what that temperature distribution should be, particularly on scales small compared to the aperture diameter. These small-scale inhomogeneities will place the ultimate limit on thermal performance. To resolve these questions we need to make measurements on comparable existing structures. We propose to do this on the 12-m antenna and also on one of the new BIMA 6-m antennas. The BIMA antennas are more appropriate since they are not in an enclosure and are more comparable in size to the proposed mmA antennas. This will be done using arrays of thermistors and we also propose to borrow the IR camera from the MMT. Typically, it is expected that temperature differences of tenths of a kelvin will be the maximum that can be tolerated.

Some methods of instrumentation need to be looked at, and experience with the quadrant detectors for the 12-m and the GBT, the laser ranger and auto-collimator for the GBT, and tiltmeters within NRAO and at other institutions should be extended.

10.1 Suggested Thermal Error Budget

For both the panels and the backing structure the thermal errors may have the same form as those due to gravity and wind loading so that their component in the error budget should be more conservative than would be obtained by quadrature addition. It is probably true, however, that the thermal and wind effects will not be maximum simultaneously since wind tends to smooth out the temperature gradients.

The values in Table IV are therefore suggested as reasonable components for the surface error and pointing:

Surface Error	Panel: Absolute Temperature	3 mm
	Panel: Thermal Gradient	3 mm
	Backing Structure: Thermal Gradient	3 mm
Pointing	Mount: Thermal Gradient (after correction)	0.25 arcsec
	Backing Structure: Thermal Gradient (after correction)	0.25 arcsec

Table IV Proposed thermal components of surface accuracy and pointing error budgets.

11 References

[1] S. von Hoerner: "Design of large steerable antennas", Ap. J. Vol. 72, No. 1, February 1967, pp. 35-47.

[2] R. N. Bracewell: *The Fourier transform and its applications*, McGraw-Hill, 1986: New York

[3] C. James: "VLA and VLBA antenna temperature measurements", VLA Test Memo., No. 160., NRAO, December 1991.

[4] J. D. Bregman and J. L. Casse: "A simulation of the thermal behaviour of the UK-NL millimeter wave telescope", Int. J. IR and Millimeter Waves, Vol. 6, No. 1, 1985, pp. 25-40.

[5] P. Raffin: "Analysis of reflector back-up structure", Submillimeter Array Tech. Memo., SAO No.51, Sept 1991.

[6] K. Akabane: "A large millimeterwave antenna", Int. J. IR and Millimeterwaves, Vol. 4, No. 5, 1983, pp. 793-808.

[7] A. Greve, M. Dan, and J. Penalver: "Thermal design and thermal behavior of mm-wavelength radio telescopes", IRAM Internal Report

[8] E. Guyer (Ed): *Handbook of applied thermal design*, McGraw-Hill, New York, 1989.

[9] J. Delannoy: "The design of high frequency antennas", IAU Coll. 131, 8-12 Oct, 1990.

[10] J. M. Payne, D. Parker and R.Bradley: "A rangefinder with fast multiple range capability", GBT Memo No. 73, NRAO, 1992

[11] R. E Hills: "Detailed results of panel development programme: I Surface finish and 'figure' ", JCMT Report ASR/MT/T/443/REH(83), July, 1983.

[12] W. J. Welch, Private communication.